Loss of migfilin expression has no overt consequences on murine development and homeostasis

Daniel V. Moik, Vaibhao C. Janbandhu and Reinhard Fässler*

Max-Planck-Institute of Biochemistry, Department of Molecular Medicine, 82152 Martinsried, Germany

*Author for correspondence (faessler@biochem.mpg.de)

Accepted 5 October 2010
Journal of Cell Science 124, 414-421

doi:10.1242/jcs.075960

Summary

Migfilin is a LIM-domain-containing protein of the zyxin family of adaptor proteins and is found at cell–matrix and cell–cell adhesion sites and in the nucleus. In vitro studies have suggested that migfilin promotes β1 integrin activity, regulates cell spreading and migration and induces cardiomyocyte differentiation. To test directly the function of migfilin in vivo, we generated a migfilin-null mouse strain. Here, we report that loss of migfilin expression permits normal development and normal postnatal aging. Fibroblasts and keratinocytes from migfilin-null mice display normal spreading and adhesion, and normal integrin expression and activation. The migration velocity and directionality of migfilin-null embryonic fibroblasts were normal, whereas the velocity of migfilin-null keratinocytes in wound scratch assays was slightly but significantly reduced. Our findings indicate that the roles of migfilin are functionally redundant during mouse development and tissue homeostasis.

Key words: Fblim1, Migfilin, Adhesion, Integrin, F-actin, Development, Zyxin family

Introduction

Cell–matrix and cell–cell adhesions are essential for the development and homeostasis of multicellular organisms. During development, cell adhesion to defined substrates or neighboring cells defines spatial identity and can induce cell fate decisions and provide migratory guidance cues. In fully developed organisms, adhesion-mediated signaling provides survival cues and regulates tissue functions. Cell adhesion to extracellular matrix (ECM) proteins is largely mediated through specific transmembrane receptors of the integrin family. Integrins are heterodimeric glycoproteins comprising α and β subunits. Each subunit consists of a large extracellular domain, a transmembrane domain and a short cytoplasmic domain. Integrins function as bidirectional signaling molecules; their affinity for ligands is regulated (integrin activation) by direct interactions of the β-subunit cytoplasmic tails with the cytoskeletal proteins talin and kindlin (inside-out signaling) (Moser et al., 2009). Following ligand binding, integrins transduce signals into cells (outside-in signaling) by forming large signaling hubs called focal adhesions (FAs), which consist of signaling and adaptor proteins that regulate actin dynamics and various intracellular signaling pathways (Hynes, 2002; Legate and Fässler, 2009).

Migfilin [encoded by filamin-binding LIM protein 1 (Fblim1)] is an adaptor protein that is recruited to FAs. It belongs to the zyxin family of LIM-domain-containing proteins (where LIM stands for Lin-11, Isl-1 and Mec-3) and comprises an N-terminal domain, without obvious sequence motifs, followed by a proline-rich region containing a nuclear export signal (NES) and three C-terminal LIM domains. The N-terminal domain of migfilin can bind to filamins, the proline-rich region to VASP (for vasodilator-stimulated phosphoprotein) (Zhang et al., 2006) and the LIM domains to kindlin-2 (FERMT2) and the transcription factor Nkx2.5 (Akazawa et al., 2004; Takafuta et al., 2003; Tu et al., 2003). Migfilin is encoded by a single gene, which can be alternatively spliced to give rise to two smaller isoforms whose biological relevance is unknown; one splice variant is called migfilin(s), which lacks the NES and the proline-rich region. The other isoform is called filamin-binding LIM protein 1 (Fblp1), which lacks the third LIM domain.

Studies with cultured cell lines have identified migfilin as an important mediator of integrin function. Small interfering RNA (siRNA)-mediated depletion of migfilin in different cell lines results in reduced integrin-mediated adhesion, spreading and migration (Tu et al., 2003; Zhang et al., 2006). Talin and the kindlins activate integrins (Montanez et al., 2008; Moser et al., 2009), whereas filamins compete with talin for binding to the cytoplasmic tails of integrins and thereby attenuate integrin activation (Kiema et al., 2006). On the basis of findings showing that migfilin can compete with β-integrin cytoplasmic tails for binding to filamins, it has been proposed that migfilin conveys its stimulating role on integrins by promoting talin binding to integrin tails, resulting in integrin activation (Ithychanda et al., 2009; Lad et al., 2008). Interestingly, overexpression of migfilin can also diminish cell migration, which was shown to depend on the proline-rich motif (Zhang et al., 2006). Furthermore, the proline-rich motif seems to be required for recruiting VASP to FAs. It is not entirely clear, however, whether recruitment of VASP plays a regulative role for modulating cell migration.

Besides its role in cell–matrix adhesions, migfilin has been shown to have several additional functions. Migfilin is found at cell–cell junctions together with β-catenin; formation of cell–cell contacts was impaired after siRNA-mediated knockdown of migfilin, as shown in a time course with keratinocytes after addition of Ca^{2+} (Gkretsi et al., 2005). Furthermore, migfilin is also present in the nucleus, where it might co-activate transcription factors including Nkx2.5 (Akazawa et al., 2004), whose activity is essential for heart morphogenesis. Finally, migfilin has also been shown to bind to c-Src, which promotes cell survival (Zhao et al., 2009).

To test directly the role of migfilin function in vivo, we used homologous recombination in embryonic stem (ES) cells to generate null alleles for the gene encoding migfilin. Surprisingly, migfilin-null mice develop and age normally. These results suggest that the role of migfilin in adhesion signaling and developmental pathways overlaps with functions of other LIM-domain-containing proteins.

Results

Migfilin-null mice have no apparent phenotype

We generated a conditional floxed (fl) allele of the gene encoding migfilin by flanking exons 2 and 3 with loxP sites (supplementary material Fig. S1A,B). Intercrossing of floxed migfilin mice with a deleter flippase removed the neomycin selection cassette and resulted in migfilin floxed mice, which expressed comparable migfilin levels in all tissues tested including heart (supplementary material Fig. S1C and data not shown). Mating migfilin floxed mice with a deleter-Cre strain removed the loxP-flanked exons, which contain the start codon of migfilin. Given that downstream ATG codons would not be in the correct reading frame, we expected to observe loss of migfilin expression. To confirm this, we performed western blotting of lung and heart lysates using an antibody raised against a peptide from the first LIM domain of migfilin. In control lysates the antibody recognized a single band at an apparent molecular mass of 50 kDa (Fig. 1A). This was larger than the predicted size calculated from the primary sequence but comparable with the reported molecular mass of human migfilin (Tu et al., 2003). We did not detect bands at molecular masses below 50 kDa, suggesting that Fblp1 or migfilin(s) was not expressed in heart and lung (Fig. 1A). As expected, migfilin protein was absent from homozygous mutant migfilin (–/–) mice and reduced in migfilin heterozygous (+/–) mice (Fig. 1A). Cre-mediated deletion of exons 2 and 3 did not significantly affect the level of the transcript encoding migfilin, as measured by quantitative RT–PCR (supplementary material Fig. S1D). Offspring from migfilin heterozygous intercrosses yielded normal numbers of migfilin-null mice, which presented no apparent defects (Fig. 1B), gained weight in the same manner as wild-type and heterozygous littermates (Fig. 1C) and were fertile.

To test whether other zyxin family members were upregulated, thereby compensating for the loss of migfilin, we performed quantitative RT–PCR and western blotting in heart and lung. We did not observe significant changes of their transcript or protein levels upon migfilin deletion (Fig. 1D,E; supplementary material Fig. S1E,F), indicating that compensatory upregulation did not occur.

Expression profile of migfilin

As migfilin-null mice did not have an obvious phenotype, we decided to analyze migfilin expression in various mouse tissues. Western blotting detected migfilin protein in heart, lung, skin, spleen, uterus and in the entire intestinal tract (Fig. 2A). In line with a previous report (Takafuta et al., 2003), migfilin levels were not detectable in platelets (supplementary material Fig. S2A). Furthermore, we could not detect migfilin in B cells and mast cells and found only very low amounts in macrophages (supplementary material Fig. S2A). Northern blotting showed a major transcript encoding migfilin of 3.2 kb in heart, lung, skin, intestinal tract, spleen and uterus (Fig. 2B). As previously reported (Akazawa et al., 2004), lung contained a second transcript with a size of approximately 6 kb (Fig. 2B). Brain, kidney, liver, skeletal muscle and thymus lacked detectable migfilin mRNAs (Fig. 2B). RT–PCR confirmed the absence of migfilin expression in brain, liver and

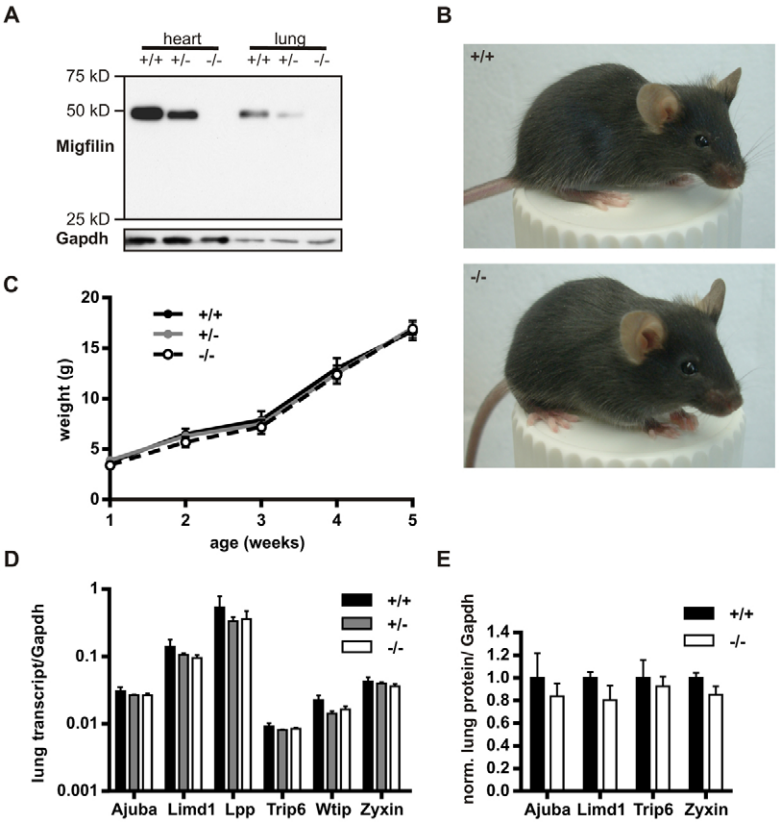

Fig. 1. Migfilin-null mice are viable and without obvious phenotype. (**A**) Western blot of migfilin expression in heart and lung from migfilin wild-type, heterozygous and null (+/+, +/– and –/–, respectively) littermates. Gapdh served as the loading control. (**B**) Wild-type and migfilin-null littermates at 4 weeks of age. (**C**) Weight-gain curve of migfilin wild-type (n=7), heterozygous (n=15) and null (n=7) littermates. (**D**) Quantitative RT–PCR analysis of the zyxin family members using total RNA isolated from migfilin wild-type, heterozygous and null lung. Transcript levels were normalized to the levels of Gapdh. Results are means + s.d. (**E**) Expression levels of the indicated proteins in wild-type and migfilin-null lungs (three animals per genotype). Band intensities of western blots were first normalized to that of Gapdh, then normalized to the wild-type expression levels. Results are means + s.d.

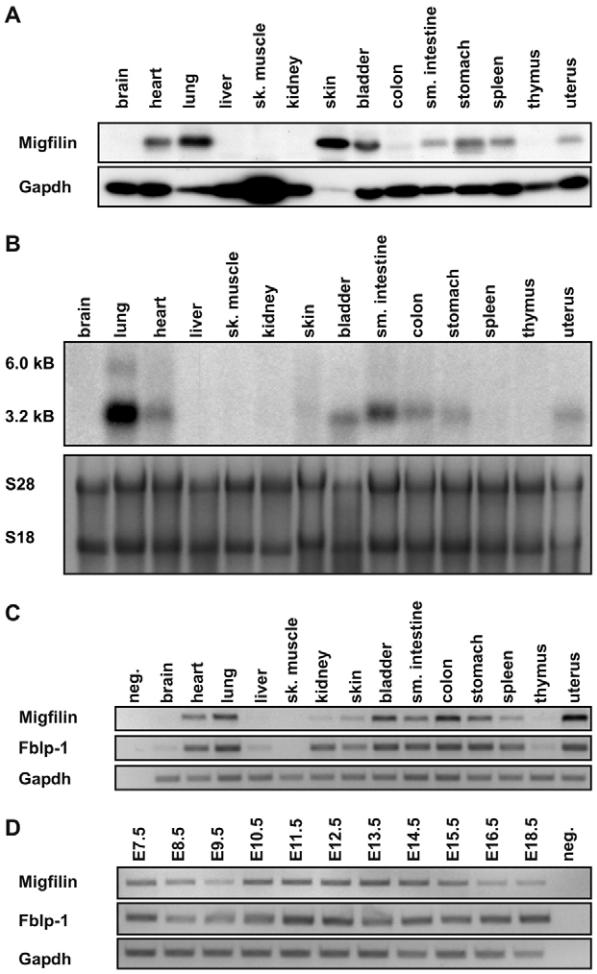

Fig. 2. Expression profile of murine migfilin. (**A**) Western blot of migfilin in different organs. Gapdh served as the loading control. (**B**) Northern blot analysis of migfilin from indicated tissues. The 28S and 18S ribosomal RNAs are shown as a loading control. (**C**) Semi-quantitative RT–PCR from the indicated tissues. The migfilin-specific primers span exons 5 and 8 and the Fblp1-specific primers span exons 6 and 7b (results are after 36 cycles for the latter) (see supplementary material Fig. S2C for a schematic of the primer positions). neg. represents a no-template control. (**D**) Semi-quantitative RT–PCR from whole embryos at the indicated embryonic age (E).

skeletal muscle and revealed only minute amounts in kidney and thymus (Fig. 2C).

The *FBLP1* transcript in humans is generated by a read-through of exon 7 into the following intron (supplementary material Fig. S2B) and thus lacks exons 8 and 9 coding for the third LIM domain. Primers specific for the equivalent murine *Fblp1* transcript (supplementary material Fig. S2C) detected very low *Fblp1* mRNA levels, as we required 36 amplification cycles to detect *Fblp1* mRNA in brain and liver (Fig. 2C). Expression of the migfilin(s) transcript could not be detected with primers flanking exons 3 and 6 (data not shown). Semi-quantitative RT–PCR with total RNA isolated from embryos of embryonic day (E) 7.5 to 18.5 (Fig. 2D) detected mRNAs encoding migfilin and Fblp1 in all stages analyzed.

Migfilin-null mice have no apparent organ abnormities

Next we carried out hematoxylin and eosin (HE) and immunofluorescence stainings of sections from various tissues. HE staining revealed no abnormalities in hearts from migfilin-null mice (Fig. 3A). Migfilin colocalized with vinculin at the intercalated discs in the wild-type heart (Fig. 3A; see also supplementary material Fig. S3A for single-color channels). Previous data implicated a nuclear localization of migfilin in cardiomycytes (Akazawa et al., 2004), which we could not confirm (Fig. 3A). As expected, migfilin expression was lost in hearts from migfilin-null mice. Although migfilin expression was lost, we found a normal distribution of vinculin (Fig. 3A; supplementary material Fig. S3A).

Despite the high expression of migfilin in the lung, we did not detect abnormalities in lungs from migfilin-null mice (Fig. 3B). Migfilin levels were high in lung epithelial cells (Fig. 3B), in mural cells of the lung vasculature (supplementary material Fig. S3B) and in residential macrophages (Fig. 3B, arrowheads; supplementary material Fig. S3C). Lung endothelial cells, visualized by endomucin co-staining, did not express detectable levels of migfilin (Fig. 3B).

The morphology of colon and kidney was unaltered in migfilin-null mice, as determined by HE staining (Fig. 3C,D), and immunofluorescence stains revealed low expression of migfilin in cryptal enterocytes and high expression in upward moving and differentiated enterocytes (Fig. 3C). Although we did not detect migfilin protein in lysates of whole kidney (Fig. 2A), migfilin levels were high in glomeruli (Fig. 3D).

Finally, apoptosis was normal in all the organs we tested (data not shown). We also could not detect changes in the levels of total Src and Src phosphoylated at Tyr416 in lung tissue lysates from migfilin-null mice (supplementary material Fig. S3D).

Migfilin-null cells display normal F-actin distribution and β1 integrin activation

Next, we isolated primary migfilin-null keratinocytes, cultured them in the presence of low levels of Ca^{2+}, to prevent differentiation, and analyzed integrin- and actin-mediated functions. Migfilin was present in FAs of wild-type keratinocytes, where it colocalized with vinculin (Fig. 4A). Migfilin-null cells developed normal FAs, in terms of number and size, which were connected to F-actin stress fibers in a manner similar to that in wild-type cells (Fig. 4B). In contrast with a previous report (Zhang et al., 2006), we found robust recruitment of VASP to vinculin-containing FAs both in migfilin-null keratinocytes (Fig. 4C,D) and in migfilin-null fibroblasts (data not shown). Addition of Ca^{2+} induced migfilin translocation to cell–cell adhesion sites, where it colocalized with vinculin (Fig. 4E). Upon Ca^{2+} treatment migfilin-null cells were also able to form cell–cell adhesions with a fine, but prominent, lining of vinculin (Fig. 4F).

We next tested whether migfilin-null cells have a normal integrin profile. The levels of integrin β1, β4, α2, α5 and αv were similar on wild-type and migfilin-null keratinocytes (Fig. 4G; supplementary material Fig. S4B). We also found normal 9EG7 binding on migfilin-null keratinocytes (Fig. 4H; supplementary material Fig. S4B) and a similar increase in 9EG7 binding on wild-type and migfilin-null keratinocytes after treatment with Mn^{2+} (Fig. 4H). These findings suggest that migfilin is required neither for maintaining the basal β1 integrin activity nor for inducing β1 integrin activation by Mn^{2+}.

Migfilin promotes the migration speed of keratinocytes

siRNA-mediated depletion of migfilin has been shown to impair integrin-mediated adhesion and spreading of human cells (Tu et

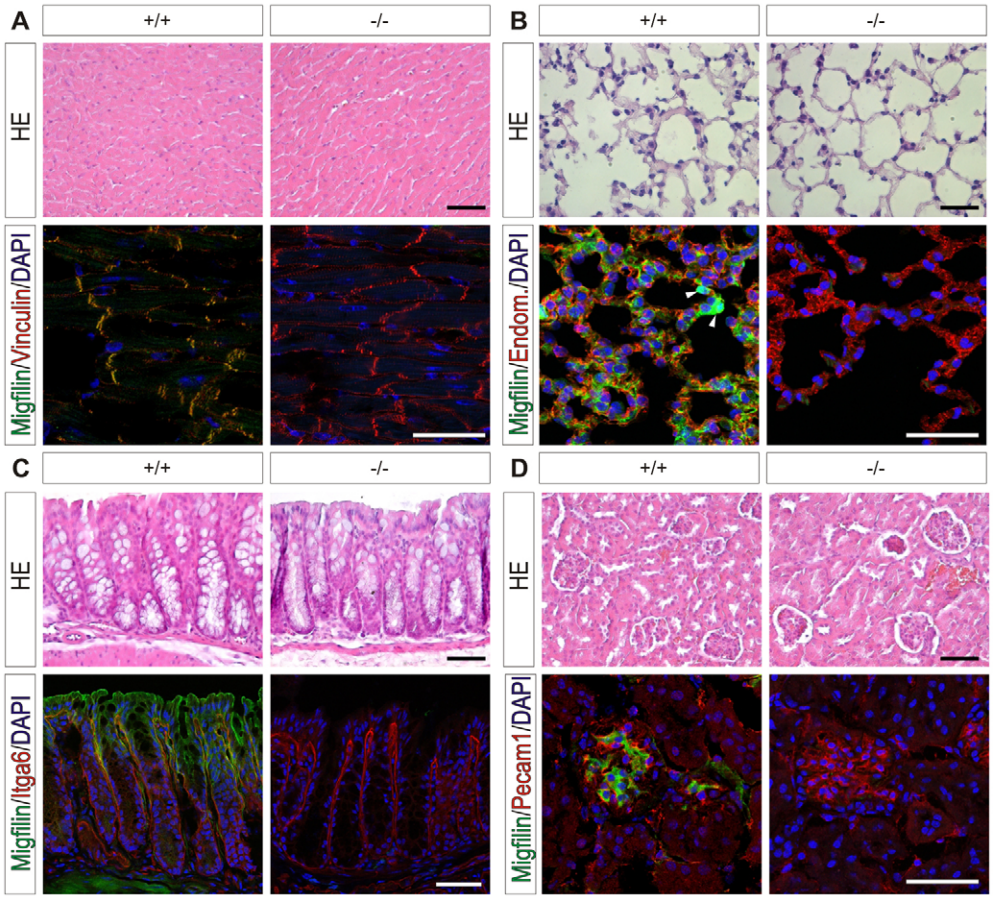

Fig. 3. Migfilin is not required for tissue homeostasis. Hematoxylin and eosin (HE) and immunofluorescence staining of migfilin wild-type (+/+) and null (–/–) heart (**A**), lung (**B**), colon (**C**) and kidney (**D**) with the indicated antibodies. Endom., endomucin. The arrowheads in B indicate residential macrophages. Scale bars: 50 μm.

al., 2003; Zhang et al., 2006). To test whether genetic ablation led to similar defects, we plated wild-type and migfilin-null keratinocytes on different substrates to compare their adhesive and spreading properties. Loss of migfilin expression did not affect adhesion to collagen I, collagen IV, fibronectin or laminin-322 (Fig. 4I). Furthermore, spreading of migfilin-null keratinocytes on a mixture of collagen I and fibronectin was also indistinguishable from that displayed in wild-type cells (Fig. 4J).

It is possible that abrupt migfilin depletion by specific siRNAs results in phenotypic changes that are not visible in the 'compensation prone' genetic model used in the present study. To test this possibility, we performed siRNA-mediated depletion of migfilin in immortalized migfilin floxed (fl/fl) mouse embryonic fibroblasts (MEFs). This resulted in an efficient knockdown of migfilin, whereas cells transfected with a scrambled control siRNA expressed normal levels of migfilin (supplementary material Fig. S5A and data not shown). To control off-target effects, we also transfected migfilin-null MEFs derived from fl/fl MEF clones with these siRNAs. Vinculin localized to FAs in both migfilin fl/fl and null MEFs transfected with either migfilin-specific or scrambled siRNAs (supplementary material Fig. S5B). Furthermore, the size and the number of FAs were similar in cells transfected with either siRNA (supplementary material Fig. S5B). Moreover, we did not find defects in cell adhesion or in spreading kinetics (supplementary material Fig. S5C,D).

Given that it has also been reported that siRNA-mediated migfilin depletion impairs cell migration (Zhang et al., 2006), we analyzed cell migration in a scratch wound assay. Whereas migfilin-null MEFs showed a migration behavior similar to that of wild-type cells (Fig. 5A; supplementary material Fig. S5E), migration velocity was reduced by 28% in migfilin-null keratinocytes when compared with that of wild-type keratinocytes ($P<0.001$; Fig. 5B; supplementary material Fig. S5F). The directionality of migration was unchanged in migfilin-null keratinocytes (Fig. 5B).

To ensure that the migration defect of migfilin-null keratinocytes was specific to migfilin loss, we retrovirally transduced migfilin-null keratinocytes with expression constructs encoding either the wild-type migfilin–GFP (green fluorescent protein) fusion protein or for the filamin-binding-deficient (D11A13 mutated) migfilin–GFP fusion protein (Ithychanda et al., 2009). The transduced cells were sorted by FACS for equal GFP levels (Fig. 5C) and the subcellular localization of the fusion proteins was analyzed. Both migfilin–GFP and migfilin(D11A13)–GFP localized to FAs (Fig. 5D). Similar to endogenous migfilin in wild-type keratinocytes (Fig. 4A), the re-expressed wild-type protein also weakly localized to F-actin stress fibers (Fig. 5E). This stress fiber localization depended on interaction with filamins as it could not be observed in cells expressing migfilin(D11A13)–GFP (Fig. 5E). Both constructs were able to rescue the defect in the migration velocity of migfilin-null keratinocytes ($P<0.001$; Fig. 5F). These findings suggest that the migfilin–filamin interaction is not required for controlling the migration speed in keratinocytes.

Discussion

Cell–ECM adhesion is important for cell shape, motility and signaling. Migfilin is an integrin-proximal adaptor localized to FAs and provides a link between integrins and the actin cytoskeleton (Takafuta et al., 2003; Tu et al., 2003). Here, we tested the role of

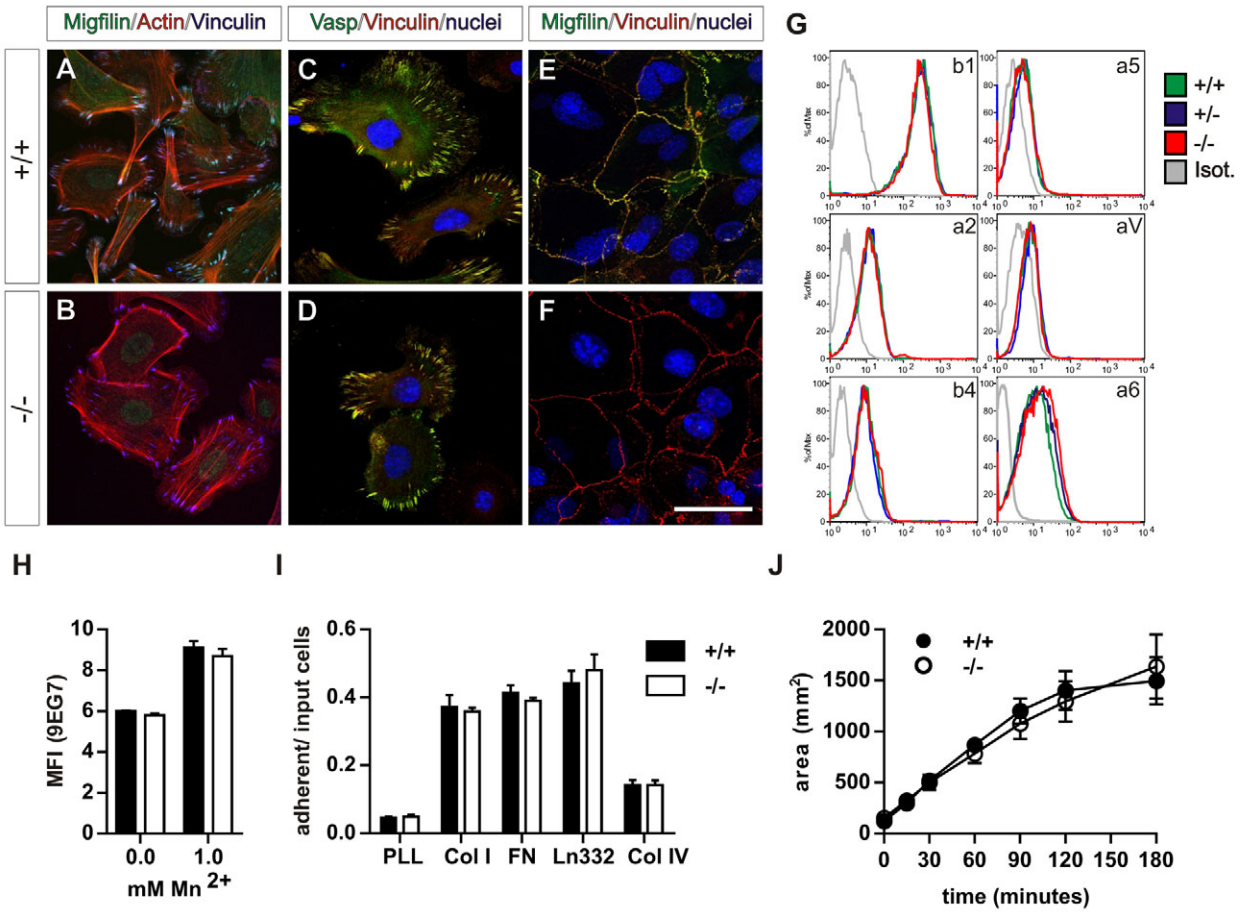

Fig. 4. Migfilin-null keratinocytes have normal integrin function. Immunofluorescence staining of primary migfilin wild-type (+/+; **A**,**C**,**E**) and null (–/–; **B**,**D**,**F**) keratinocytes for migfilin (green), F-actin (red) and vinculin (blue) (panels A and B); for VASP (green), vinculin (red) and nuclei (blue) (panels C and D); and for migfilin (green), vinculin (red) and nuclei (blue) after Ca^{2+} treatment for 24 hours (panels E and F). Scale bar: 20 µm. (**G**) Primary keratinocytes from migfilin wild-type, heterozygous (+/–) and null mice were stained with antibodies against the indicated integrin subunits and analyzed by flow cytometry. Isot., isotype control. (**H**) Flow cytometry of primary keratinocytes stained with the monoclonal antibody 9EG7 before and after treatment with 1 mM Mn^{2+}. Normalized mean fluorescence intensity (MFI) values are shown. Data are measurements from a single representative experiment repeated three times and are means + s.d. (**I**) Cell adhesion assay with primary migfilin wild-type and null keratinocytes on poly-L-lysine (PLL), collagen I (Col I), fibronectin (FN), laminin 322 (Ln322) and collagen IV (Col IV). Results are the means + s.e.m. for four replicates. (**J**) Spreading kinetics of primary keratinocytes on FN+Col I when visualized by time-lapse microscopy. A total of ten cells per genotype were analyzed; the cell area was measured using ImageJ. Results are means ± s.e.m.

migfilin in vivo by genetically ablating the gene encoding migfilin. Unexpectedly, we found that migfilin is dispensable for development and tissue maintenance.

The wide expression pattern of migfilin suggested a role for this FA protein in several organs. Although high levels were found at the intercalated discs of cardiomyocytes and in smooth muscle cells, migfilin was not detected in skeletal muscle. Similarly, some epithelia, such as epidermis, lung and intestine, expressed high levels of migfilin, whereas in others, such as in the epithelium of the esophagus, tongue or mammary gland, it could not be detected (data not shown). However, regardless of the migfilin expression level in the different tissues, we were unable to detect abnormalities in migfilin-null organs, including changes in cell survival.

It has been suggested that migfilin promotes activation of integrin β1 in vitro (Ithychanda et al., 2009); however, we observed no change in activation of integrin β1 upon eliminating migfilin expression in vivo. This also holds true for all previously published in vitro findings regarding cell–matrix adhesion and cell spreading. In line with a previous observation (Zhang et al., 2006), we noticed a reduction in the migration speed of migfilin-null keratinocytes in scratch assays. Migfilin-null fibroblasts, however, did not display this defect. Previous cell culture studies demonstrated that both siRNA-mediated depletion, as well as overexpression, of migfilin reduce migration speed (Zhang et al., 2006). It has been proposed that a diminished localization of VASP to FAs might cause the diminished migration speed. Clearly, this observation cannot explain the defect in primary cells as we did not observe defects in VASP localization after genetic ablation of migfilin in keratinocytes.

We do not know why migration velocity is reduced in migfilin-null keratinocytes. Neither polarity nor directionality of migration was affected, which excludes a requirement for migfilin in initiating or maintaining a polarized lamellipodium (Harms et al., 2005). Integrin activation and keratinocyte adhesion were also unchanged, precluding increased integrin activity as a cause for the reduced migration speed. We can also exclude abnormal distribution or reduced levels of p130Cas (Bcar1) in nascent FAs as cause for the reduced migration speed (data not shown). Such a reduced p130Cas level leading to diminished Rac1 activity was shown to be causative

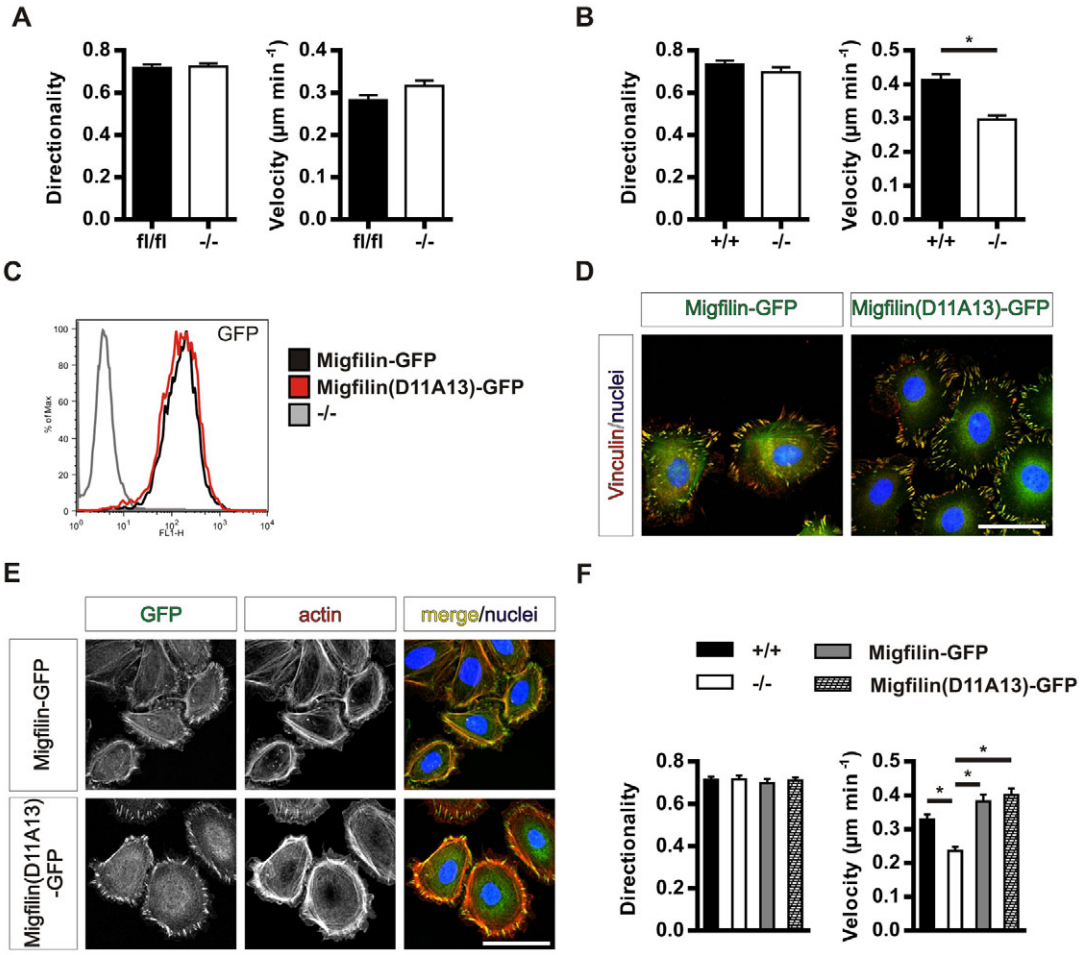

Fig. 5. Migfilin-null keratinocytes have a reduced migration velocity. (**A**) Monolayers of migflin (fl/fl) and null (–/–) MEFs were scratch wounded and scratch closure was visualized by time-lapse microscopy. Migration was analyzed by tracking single cells using ImageJ. Data shown are measurements from three experiments and are mean + s.e.m. for 30 tracks. (**B**) Migfilin wild-type (+/+) and null primary keratinocytes were grown to confluence, wounded and analyzed as in A. Data shown are measurements from three experiments and are means + s.e.m. for 40 keratinocyte tracks. **P*<0.001. (**C**) Representative FACS plot of migflin-null immortalized keratinocytes expressing migfilin–GFP or migfilin(D11A13)–GFP. (**D**) Immunofluorescence staining for vinculin (red) and nuclei (blue) of migfilin-null keratinocytes re-expressing migfilin–GFP or migfilin(D11A13)–GFP. The GFP signal is shown in green. Scale bar: 20 µm. (**E**) Immunofluorescence staining for F-actin (red) and nuclei (blue) of migfilin-null keratinocytes re-expressing migfilin–GFP or migfilin(D11A13)–GFP. The GFP signal is green in the 'merge' image. The single channels for the GFP and actin signal are also shown. Scale bar: 20 µm. (**F**) Monolayers of immortalized migfilin wild-type and null, and migfilin-null keratinocytes rescued with either migfilin–GFP or migfilin(D11A13)–GFP, were scratch wounded and analyzed as in A. Data shown are measurements from three experiments and are means + s.e.m. for 40 keratinocyte tracks. **P*<0.001.

for the migration defect in Ajuba-deficient cells (Pratt et al. 2005). The migration defect was specific to the loss of migfilin as re-expression of migfilin in migfilin-null keratinocytes restored the wild-type migration speed. Interestingly, re-expression of a filamin-binding-deficient migfilin mutant was also able to rescue the migration speed. Clearly, future studies are required to unravel how migfilin affects migration.

Several zyxin family members can translocate to the nucleus, where they influence gene expression (Hervy et al., 2006). Migfilin has also been shown to be present in nuclei and, furthermore, has an NES for exiting the nuclear compartment (Akazawa et al., 2004). These findings, together with the observation that migfilin can interact with the transcription factor Nkx2.5, led to the proposal that migfilin might be required for heart development (Akazawa et al., 2004). However, genetic ablation of migfilin resulted neither in abnormal heart development nor in structural heart defects or heart failure. As we never observed nuclear accumulation of migfilin in heart or any other tissue, as analyzed by immunofluorescence staining, nuclear translocation of migfilin is either a transient event or it occurs only under specific conditions such as tissue stress.

The zyxin gene family consists of seven members in mammals. Although we could demonstrate that none of these members was upregulated in the absence of migfilin expression, functional redundancy could serve as the explanation for the lack of phenotype. Flies have two zyxin family members and thus less possibility for redundancy. This might explain why depletion of one of the two zyxin family members in flies induces pharate lethality (Das Thakur et al., 2010). Genetic studies on different zyxin family members in mice have so far revealed that single genetic ablations allow normal development and tissue homeostasis; ablations of migfilin (the present study), ajuba (Pratt et al., 2005), limd1 (Feng et al., 2007) and zyxin allow mice to develop normally

(Hoffman et al., 2003), although Lpp-null mice show slightly reduced female viability and fertility (Vervenne et al., 2009). The functions of ajuba and limd1 have been further elucidated by challenging the mutant mice in disease models or by drug treatment. These studies have revealed that ajuba promotes activation of nuclear factor κB (NF-κB) after stimulation with interleukin-1 (Feng and Longmore, 2005) and that limd1 can act as a tumor suppressor (limd1-null mice are more prone to the development of lung cancer) (Sharp et al., 2008). It is therefore possible that zyxin family members have specialized roles in dealing with cellular or physiological stress. The presence of such potential non-compensatable functions must be addressed in the future by subjecting migfilin-null mice to different pathological situations.

Materials and Methods

Mouse generation

Migfilin cDNA was obtained from IMAGE clone no. 3257486. A single-nucleotide polymorphism resulting in the mutation I159R was reversed by site-directed mutagenesis (Stratagene). The cDNA was cloned into pBluescript II SK (Stratagene). Final constructs were confirmed by DNA sequencing. Details of the cloning of the targeting construct and mouse generation are available from the corresponding authors on request. In brief, full-length migfilin cDNA was used to generate a radiolabeled probe. This was then used to isolate a *Spe*I fragment, including exons 1 to 3 of the gene encoding migfilin and the flanking arms of the targeting construct, from a 129/Sv RPCI mouse PAC library 21 clone. A loxP site was inserted 5′ of exon 2, and a loxP site together with an frt-flanked neomycin selection cassette was inserted 3′ of exon 3. The linearized targeting vector was electroporated into R1 mouse ES cells, which were selected with G418. Surviving clones were analyzed for homologous recombination by Southern blotting using an external probe (Fässler and Meyer, 1995). Three clones showing successful homologous recombination were injected into blastocysts, which were then transplanted into foster mice. Chimeras derived from two clones gave germline transmission. Mice were kept at the MPI of Biochemistry animal facilities in accordance with Bavarian animal welfare laws.

Southern and northern blotting

For Southern blotting (SB), 15 μg of DNA was separated on an agarose gel and transferred onto Hybond N+ membranes (GE Healthcare). For northern blotting (NB), 10 μg of total RNA extracted with TRIzol (Invitrogen) was separated on a denaturing agarose gel and transferred onto Hybond N+ membranes (GE Healthcare). Full-length migfilin cDNA was excised from the pBS-Migfilin(SK) vector and radiolabeled with [α-^{32}P]CTP using a RediPrime II DNA labeling kit (GE Healthcare). Membranes were hybridized overnight at 65°C in Church buffer [250 mM Na_2HPO_4, 0.34% (v/v) H_3PO_4, pH 7.4, 7.0% (w/v) SDS, 1.0% (w/v) BSA and 0.1 g of sheared salmon sperm/l], and were then washed and exposed to Kodak Biomax MS screens for 1–8 days at –80°C .

RT–PCR

TRIzol-extracted total RNA (2 μg) was used for first-strand cDNA synthesis, using SuperScript III reverse transcriptase according to the manufacturer's protocol (Invitrogen), with random hexamer primers. Specific cDNA fragments were amplified using the following primers: migfilin forward (fwd), 5′-CAGAGAGAGAAGTG-TCCACG-3′ and reverse (rev), 5′-GATTCTCGCAGATGCTGCAC-3′; Fblp1 fwd, 5′-GTTGGCTGGACAGAGATTCTA-3′ and rev, 5′-CATTCCCGAAGCCCCAGTC-3′; glyceraldehyde-3-phosphate dehydrogenase (Gapdh) fwd, 5′-GGTGTGAA-CCACGAGAAATATG-3′ and rev, 5′-CAGTGAGCTTCCCGTTCAG-3′; migfilin(s) fwd, 5′-GATGTAGCCGTGAGTGAGG-3′ and rev, 5′-CAGGCTTGTGACAGA-AACCAC-3′. Migfilin(s) primers produce two amplicons, one specific for migfilin(s) with a size of a 207 nt and a second one specific for migfilin and *Fblp* with a size of 505 nt. The latter amplicons are suppressed by shortening the amplification cycle during PCR. Primers used to amplify zyxin family transcripts were: ajuba-exon1 fwd, 5′-GAGTCTCCTGGTCCCTTCG-3′ and ajuba-exon3 rev, 5′-CTTCCTCACA-GTAGACAGAGC-3′; Limd1-exon1 fwd, 5′-CCTCACCCAGCGTCTGG-3′ and Limd1-exon4 rev, 5′-GTCCATGATCAGGTGTCCAC-3′; Lpp-exon5 fwd, 5′-CCAGTTGTTGCTCCGAAACC-3′ and Lpp-exon7 rev, 5′-CCAAGATGC-TGGTCAAGGAG-3′; Trip6-exon3 fwd, 5′-TGGCAGTCTGGATGCTGAG-3′ and Trip6-exon4 rev, 5′-GCCACCTTCACTTGTACAGG-3′; Wtip-exon2 fwd, 5′-GGCATCTACGGAGCGAGG-3′ and Wtip-exon5 rev, 5′-GCAGCGGAAGCAG-CCTGG-3′; and zyxin-exon3 fwd, 5′-CCATTCCCCCCTGCTCCT-3′ and zyxin-exon5 rev, 5′-GGCAACTGGTGGGGGTAC-3′.

Antibody generation

A migfilin-specific peptide sequence (CVSPRELAVEAMKRQY; residues 192–206) located within LIM domain 1 was coupled to Imject Maleimide Activated mcKLH (Pierce Biotechnology) and used to immunize rabbits. The resulting serum was subsequently affinity-purified using a SulfoLink Kit (Pierce Biotechnology). Affinity purified antibodies were eluted using 100 mM glycine buffer, pH 2.7, and dialyzed against PBS.

Western blotting

Cells or tissues from adult C57BL/6 mice were homogenized in RIPA buffer, pH 7.6 [150 mM NaCl, 50 mM Tris-HCl, pH 7.6, 5 mM EDTA, pH 8.0, 0.1% SDS, 1.0% (w/v) sodium deoxycholate, 1.0% (v/v) Triton X-100 and phosphatase inhibitor cocktails P1 and P2; all purchased from Sigma] with Complete protease inhibitors (Roche). A total of 20 to 50 μg of protein per lane was separated on a polyacrylamide gel and transferred onto a PVDF membrane (Millipore). Membrane blocking and antibody dilution were performed with Tris-buffered saline (TBS), pH 7.6, supplemented with 5% (w/v) skimmed milk powder (Fluka) and 0.1% Tween 20 (Serva). Subsequently, membranes were incubated for 1 hour at room temperature or overnight at 4°C with antibodies against migfilin (self-made), actin (Sigma), Src (Invitrogen), Src phosphorylated at Tyr419 (Cell Signaling), zyxin (Abcam) or Gapdh (Chemicon). Anti-Trip6 antiserum was provided by Mary Beckerle (University of Utah, Salt Lake City, UT), and anti-Ajuba and anti-Limd1 antisera were provided by Gregory Longmore (Washington University, St Louis, MO). Appropriate HRP-coupled secondary antibodies (BioRad) were applied for 1 hour at room temperature followed by enhanced chemiluminescence (ECL) detection (Western Lightning, PerkinElmer).

Cell culture

Primary keratinocytes were isolated from mice at the telogen phase of the hair cycle. Mice were killed, shaved and skinned. Then the muscle and fatty layer were scraped off, and the skin was incubated for 1 hour in Dulbecco's phosphate-buffered saline (PBS) supplemented with 0.8% trypsin (Gibco) at 37°C. Afterwards the epidermis was peeled off the underlying dermis and manually dissociated. The resulting suspension was filtered through a 45-μm nylon mesh. Cells were seeded and maintained at 37°C under a 5% CO_2 atmosphere in growth medium [Spinner's MEM supplemented with 5 mg of insulin/l, 10 mg of EGF/l (Roche), 10 mg of transferrin/l, 10 μM phosphoethanolamine, 10 μM ethanolamine, 0.36 mg of hydrocortisone/l (Calbiochem), 0.3 g of glutamine/l, 100 units penicillin/ml, 100 mg of streptomycin/l, 45 μM $CaCl_2$ and 8% (v/v) chelated fetal calf serum (FCS)]. For differentiation, keratinocytes were cultured in growth medium containing 1 mM $CaCl_2$. For spontaneous immortalization, keratinocytes were maintained as above, at high confluency, for 2 months. When colonies of immortalized keratinocytes appeared, they were pooled and expanded.

For generation of the migfilin(D11A13)–GFP expression construct, migfilin cDNA was mutated with the Quickchange kit (Stratagene) using primers 5′-GAGAAA-AGGGTGGCCGACTCTGCTTTCATCACCCTGGCA-3′ and 5′-TGCCAGGG-TGATGAAAGCAGAGTCGGCCACCCTTTTCTC-3′. Successful mutagenesis was confirmed by sequencing. Both wild-type and mutant migfilin cDNA were cloned into pEGFP-N1 (Clontech) and subsequently into pCLMFG-MCS for generating the viral supernatants used to infect the immortalized migfilin-null keratinocytes. Cells expressing migfilin–GFP or migfilin(D11A13)–GFP were sorted using a FACS method for equal GFP levels.

Mouse embryonic fibroblasts (MEFs) were isolated from E13.5 embryos by standard methods. Immortalization was achieved by retroviral transduction of SV40 large T antigen and immortalized MEFs were subsequently cloned. Migfilin-null MEFs were derived from migfilin fl/fl MEFs by adenoviral Cre transduction followed by cloning. MEFs were maintained at 37°C under a 5% CO_2 atmosphere in Dulbecco's modified Eagle's medium (DMEM) with 4 mM glutamax, 100 units/ml penicillin and 100 mg of streptomycin/l and supplemented with 10% v/v FCS.

In some experiments, culture dishes were coated with ECM molecules as indicated. The ECM molecules used were collagen I, collagen IV, fibronectin or laminin-322 (kindly provided by Monique Aumailley, University of Cologne, Cologne, Germany). Unless noted otherwise, all cell culture reagents were purchased from Invitrogen or Sigma.

Adhesion assays

Adhesion assays were conducted in 96-well plates. Quadruplet wells were coated with the substrate overnight at 4°C. Nonspecific adhesion was assayed in wells coated with 1% BSA in PBS. Before the assay, the coating substrate was washed out and the wells were blocked with 1% BSA in PBS. A total of 40,000 cells per well were added in Spinner's MEM supplemented with 40 μM $CaCl_2$ and 2 mM glutamine. After 30 minutes at 37°C under a 5% CO_2 atmosphere, the wells were washed three times with PBS and substrate solution (3.8 mM 4-nitrophenyl *N*-acetyl-β-D-glucosaminide, 0.25% Triton X-100 and 50 mM sodium citrate, pH 5.0) was added. After an overnight incubation at 37°C, 1.5 volumes of stop solution (50 mM glycine and 5 mM EDTA, pH 10.4) was added and absorption was measured at 405 nm.

Spreading and scratch wound healing assays

Cell spreading and migration were assayed with a live-cell imaging setup consisting of a microscope (Axiovert; Carl Zeiss MicroImaging) equipped with a ×10 0.3NA objective, motorized scanning table (Märzhäuser) and a stage incubator (EMBL Precision Engineering) at 37°C and under 5% CO_2 atmosphere. Images were captured

with a cooled charge-coupled-device camera (MicroMAX; Roper Scientific) using the MetaMorph software (Universal Imaging) for microscope control and data acquisition.

For spreading analysis, cells were added to pre-equilibrated culture dishes and image acquisition was started immediately. Images were collected every 5 minutes. Cell area over time was measured using ImageJ software (National Institutes of Health). The data shown were generated by randomly choosing ten cells per genotype from a representative experiment, which was repeated three times.

For migration analysis, cells were treated with 4 mg of mitomycin C/l (Sigma), to abolish proliferation, and were seeded and allowed to achieve confluency overnight. The resulting monolayer was scratched using a 1-ml plastic pipette tip. Image acquisition was started after 1 hour and images were collected every 10 minutes for up to 30 hours. Cells at the wound edge were chosen randomly and tracked with the manual tracking plug-in from ImageJ. The resulting tracks were analyzed for directionality and velocity using the 'cell migration and chemotaxis' tool (Ibidi). The data shown were generated from experiments that were repeated three times.

siRNA-mediated knockdown

Migfilin fl/fl and the derived migfilin-null MEFs were plated to ~60–70% confluency and cultured as described above. After 24 hours, MEFs were transfected with scrambled control siRNA (siScr, 5′-GAUGAAACGCGUAACAGAU-3′) or with siRNA targeting migfilin (siMig, 5′-GAAGGAAUUUCCACGGAA-3′, Sigma) using Lipofectamine 2000 in Opti-MEM I (both by Invitrogen) according to the manufacturer's protocol. After 6 hours, the medium was changed to normal growth medium and MEFs were cultured for an additional 48 hours before further assays were conducted.

Flow cytometry

Freshly isolated primary keratinocytes were stained directly with primary antibodies for 10 minutes on ice, and after washing were then stained with secondary antibody for 10 minutes on ice. After washing, cells were resuspended in PBS containing BSA and propidium iodide. Immortalized keratinocytes were trypsinized and treated as described above. Flow cytometry was conducted on a FACSCalibur or FACSAria flow cytometer (BD). Antibodies were purchased from BD (clone 9EG7, which detects active integrin β1, and against integrins β1, α2, α5, α6 or αV) or Serotec (against integrin β4).

Immunofluorescence

Cryosections from frozen adult and embryonic tissues were prepared and embedded according to standard protocols. All tissues sections, except heart, were fixed for 10 minutes in 3.7% paraformaldehyde (PFA) in PBS, then permeabilized for 3 minutes with 0.1% Triton X-100 in PBS and blocked for 1 hour in 5% BSA in PBS. Heart sections were fixed for 10 minutes in acetone at –20°C and blocked as described above. Cells were grown on glass coverslips coated with fibronectin (5 mg/l, Calbiochem) and then fixed with PFA and blocked as described above. Antibodies were used against vinculin (Sigma), migfilin (self-made), endomucin (Santa Cruz Biotechnology), integrin α6, Mac1, Pecam1 (all by BD Pharmingen) and VASP (Cell Signaling). Appropriate fluorophore-labeled secondary antibodies were used to detect primary antibodies. Alexa-Fluro-546-labelled phalloidin (Invitrogen) was used to visualize F-actin. Slides were mounted in Elvanol. Pictures were taken with a TCS SP2 AOBS confocal laser-scanning microscope (Leica).

Statistics

All data are given as a mean value with the standard error of the mean (s.e.m.) or standard deviation (s.d.) as indicated. Statistical significance was tested with a non-paired two-tailed Student's *t*-test.

We thank Monique Aumailley for providing laminin-332, Mary Beckerle for Trip6 antiserum and Greg Longmore for antisera against Ajuba and Limd1. We are grateful to Markus Moser and Siegfried Ussar for help with design of the migfilin floxed allele. This work was supported by the Max-Planck Society.

Supplementary material available online at
http://jcs.biologists.org/cgi/content/full/124/3/414/DC1

References

Akazawa, H., Kudoh, S., Mochizuki, N., Takekoshi, N., Takano, H., Nagai, T. and Komuro, I. (2004). A novel LIM protein Cal promotes cardiac differentiation by association with CSX/NKX2-5. *J. Cell Biol.* **164**, 395-405.

Das Thakur, M., Feng, Y., Jagannathan, R., Seppa, M. J., Skeath, J. B. and Longmore, G. D. (2010). Ajuba LIM proteins are negative regulators of the hippo signaling pathway. *Curr. Biol.* **20**, 657-662.

Fässler, R. and Meyer, M. (1995). Consequences of lack of beta 1 integrin gene expression in mice. *Genes Dev.* **9**, 1896-1908.

Feng, Y. and Longmore, G. D. (2005). The LIM protein Ajuba influences interleukin-1-induced NF-kappaB activation by affecting the assembly and activity of the protein kinase Czeta/p62/TRAF6 signaling complex. *Mol. Cell. Biol.* **25**, 4010-4022.

Feng, Y., Zhao, H., Luderer, H. F., Epple, H., Faccio, R., Ross, F. P., Teitelbaum, S. L. and Longmore, G. D. (2007). The LIM protein, Limd1, regulates AP-1 activation through an interaction with Traf6 to influence osteoclast development. *J. Biol. Chem.* **282**, 39-48.

Gkretsi, V., Zhang, Y., Tu, Y., Chen, K., Stolz, D. B., Yang, Y., Watkins, S. C. and Wu, C. (2005). Physical and functional association of migfilin with cell-cell adhesions. *J. Cell Sci.* **118**, 697-710.

Harms, B. D., Bassi, G. M., Horwitz, A. R. and Lauffenburger, D. A. (2005). Directional persistence of EGF-induced cell migration is associated with stabilization of lamellipodial protrusions. *Biophys. J.* **88**, 1479-1488.

Hervy, M., Hoffman, L. and Beckerle, M. C. (2006). From the membrane to the nucleus and back again: bifunctional focal adhesion proteins. *Curr. Opin. Cell Biol.* **18**, 524-532.

Hoffman, L. M., Nix, D. A., Benson, B., Boot-Hanford, R., Gustafsson, E., Jamora, C., Menzies, A. S., Goh, K. L., Jensen, C. C., Gertler, F. B. et al. (2003). Targeted disruption of the murine zyxin gene. *Mol. Cell. Biol.* **23**, 70-79.

Hynes, R. O. (2002). Integrins: bidirectional, allosteric signaling machines. *Cell* **110**, 673-687.

Ithychanda, S. S., Das, M., Ma, Y. Q., Ding, K., Wang, X., Gupta, S., Wu, C., Plow, E. F. and Qin, J. (2009). Migfilin, a molecular switch in regulation of integrin activation. *J. Biol. Chem.* **284**, 4713-4722.

Kiema, T., Lad, Y., Jiang, P., Oxley, C. L., Baldassarre, M., Wegener, K. L., Campbell, I. D., Ylanne, J. and Calderwood, D. A. (2006). The molecular basis of filamin binding to integrins and competition with talin. *Mol. Cell* **21**, 337-347.

Lad, Y., Jiang, P., Ruskamo, S., Harburger, D. S., Ylanne, J., Campbell, I. D. and Calderwood, D. A. (2008). Structural basis of the migfilin-filamin interaction and competition with integrin {beta} tails. *J. Biol. Chem.* **283**, 35154-35163.

Legate, K. R. and Fässler, R. (2009). Mechanisms that regulate adaptor binding to beta-integrin cytoplasmic tails. *J. Cell Sci.* **122**, 187-198.

Montanez, E., Ussar, S., Schifferer, M., Bosl, M., Zent, R., Moser, M. and Fassler, R. (2008). Kindlin-2 controls bidirectional signaling of integrins. *Genes Dev.* **22**, 1325-1330.

Moser, M., Legate, K. R., Zent, R. and Fassler, R. (2009). The tail of integrins, talin, and kindlins. *Science* **324**, 895-899.

Pratt, S. J., Epple, H., Ward, M., Feng, Y., Braga, V. M. and Longmore, G. D. (2005). The LIM protein Ajuba influences p130Cas localization and Rac1 activity during cell migration. *J. Cell Biol.* **168**, 813-824.

Sharp, T. V., Al-Attar, A., Foxler, D. E., Ding, L., de A Vallim, T. Q., Zhang, Y., Nijmeh, H. S., Webb, T. M., Nicholson, A. G., Zhang, Q. et al. (2008). The chromosome 3p21.3-encoded gene, LIMD1, is a critical tumor suppressor involved in human lung cancer development. *Proc. Natl. Acad. Sci. USA* **105**, 19932-19937.

Takafuta, T., Saeki, M., Fujimoto, T. T., Fujimura, K. and Shapiro, S. S. (2003). A new member of the LIM protein family binds to filamin B and localizes at stress fibers. *J. Biol. Chem.* **278**, 12175-12181.

Tu, Y., Wu, S., Shi, X., Chen, K. and Wu, C. (2003). Migfilin and Mig-2 link focal adhesions to filamin and the actin cytoskeleton and function in cell shape modulation. *Cell* **113**, 37-47.

Vervenne, H. B., Crombez, K. R., Delvaux, E. L., Janssens, V., Van de Ven, W. J. and Petit, M. M. (2009). Targeted disruption of the mouse Lipoma Preferred Partner gene. *Biochem. Biophys. Res. Commun.* **379**, 368-373.

Zhang, Y., Tu, Y., Gkretsi, V. and Wu, C. (2006). Migfilin interacts with vasodilator-stimulated phosphoprotein (VASP) and regulates VASP localization to cell-matrix adhesions and migration. *J. Biol. Chem.* **281**, 12397-12407.

Zhao, J., Zhang, Y., Ithychanda, S. S., Tu, Y., Chen, K., Qin, J. and Wu, C. (2009). Migfilin interacts with Src and contributes to cell-matrix adhesion-mediated survival signaling. *J. Biol. Chem.* **284**, 34308-34320.